# OptiTrack-aided Supervised Learning for Neural Network Based Ultra-wideband Ranging Bias Correction

Changwei Chen Solmaz S. Kia, *senior member, IEEE*
*University of California Irvine*

***Abstract*— This paper proposes a learning-based bias correction method to improve the measurement accuracy of the ultra-wideband (UWB) ranging sensors. Our approach uses multiple artificial neural networks (ANNs) for the UWB line-of-sight (LoS) and non-line-of-sight (NLoS) measurements scenarios discrimination and bias-free range prediction for each scenario respectively. The innovation in our work includes a novel set of features that are readily available on low-cost UWB ranging sensors to train the ANNs and collecting the training data via the OptiTrack motion capture camera system. OptiTrack system allows us to collect measurements between an UWB sensor mounted on a moving pedestrian and a set of stationary UWB sensors, resulting in collecting a diverse set of training data at various relative poses between the UWB transceivers. The effectiveness of our OptiTrack-aided supervised learning-based UWB bias correction (OLUC) method is demonstrated via a set of pedestrian localization experiments, which show our method results in significantly improved localization accuracy.**

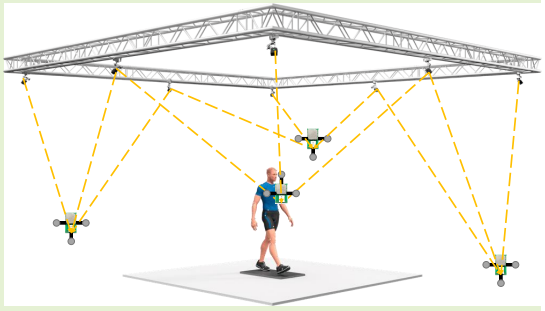

***Index Terms*— UWB ranging, OptiTrack, machine learning, bias correction, neural network, localization**

## I. Introduction

Radio frequency (RF) communication-based localization techniques that use Time-of-Flight (ToF) ranging [1] between a transceiver on a mobile agent (e.g., pedestrians, unmanned aerial vehicles, and mobile robots) and a set of pre-installed beacon transceivers with known locations have been proposed as a practical solution for some applications such as asset tracking indoors where the Global Navigation Satellite System (GNSS) fails to provide accurate location. Among various RF signals for ranging, the Ultra-wideband (UWB) signal has received considerable attention for indoor localization applications [2], [3]. The short impulse of the UWB signals makes them less susceptible to interfering with each other and with other coexisting radio signals such as WiFi and Bluetooth [4]. The low power emission of the UWB signals also makes them energy-efficient [4]. Comparing to radar-based techniques, UWB has better accuracy ratios and higher signal-to-noise ratios [5]–[7]. Other favorable attributes include low cost, high time-resolution, and obstacle-penetrating ranging [5], [8]–[10] that enables non-line-of-sight (NLoS) ranging. Nevertheless, a number of challenges should still be resolved to ensure high accuracy UWB ranging. NLoS and multi-path radio propagation can lead to biased measurements due to the time increment for the signals to penetrate through obstructions or travel a longer non-direct path [11], [12]. It is also observed that the line-of-sight (LoS) UWB range measurements exhibit spatially varying bias due to the relative pose and orientation between UWB sensors [13] and their antenna radiation patterns [14]. Therefore, to ensure UWB localization accuracy, it is critical to account for the bias in the UWB range measurements before using them. Bias correction/compensation in the UWB ranging is not fully resolved and is an active area of research.

NLoS UWB ranging bias is often significant. To deal with UWB NLoS bias, some localization approaches rely on identifying NLoS signals and avoid using them for ranging [15]–[18].

However, excluding NLoS range measurements means that in complex and cluttered indoor environments where most of the measurements are obtained in the NLoS cases, we should deploy a large number of beacon transceivers to increase the probability of taking LoS measurements if we want to implement the LoS-only UWB ranging. Still, NLoS scenarios may not be fully avoidable because of mobile obstacles in the environment, such as pedestrians.

There are mainly two approaches in the literature to handle

The authors are with the Mechanical and Aerospace Eng. Dept. of Univ. of California Irvine, CA 92697, USA, changwc3,solmaz@uci.edu. This work was supported by the U.S. Dept. of Commerce, National Institute of Standards and Technology award 70NANB17H192.

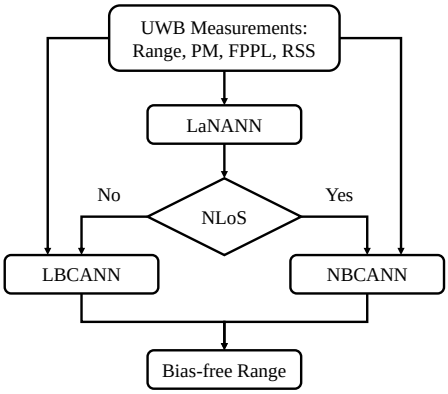


Fig. 1 – The diagram of our learning-based UWB LoS and NLoS classification and bias correction method. PM: Power Metric, FPPL: First Path Power Level, RSS: Received Signal Strength, LaNANN: Line-of-sight and Non-line-of-sight artificial neural network, NLoS: Non-line-of-sight, LBCANN: Line-of-sight bias compensation artificial neural network, LaNANN: Non-line-of-sight bias compensation artificial neural network.

the bias in UWB range measurements. The first one is the model-based bias correction, where the bias is either modeled with a known analytical expression [19]–[21] or considered as a parameter in the state vector to be jointly estimated with other state parameters [22]–[26]. In practice, however, the prior information about the bias may not be available accurately beforehand. The second approach is the model-free bias correction using ML techniques. The main idea is using ML methods, e.g., support vector machine (SVM) [27], k-nearest neighbor (k-NN) [28], deep neural network (DNN) [29] for LoS and NLoS classification and to learn the bias in NLoS scenarios.The corresponding features for classification and learning the bias include the channel impulse responses, the energy of the received signal, the maximum amplitude of the received signal, and the mean excess delay. However, the channel impulse response features are not readily available in low-cost UWB devices [30]. Moreover, complex learning models with large number of features also come with high computational complexity, which may limit use of this models in the embedded systems. A lightweight learning method to estimate the UWB ranging bias in NLoS was proposed in [31]. But this method uses the relative pose as a feature input to ML, which may not easily be available in every localization application. The method in [31] in fact is proposed for UWB time difference of arrival (TDOA)-based localization which involves three UWB radios instead of two, which is used in the ToF-based localization applications.

In this paper, we propose a novel bias correction framework for both LoS and NLoS UWB ranging via low-cost UWB transceivers. Our method, is depicted in Fig. 1. The novel features we use in our ML-based framework are the first path power level (FPPL), the received signal strength (RSS), the power metric (PM), and the raw range measurement, which are readily available on low-cost UWB transceivers such as the popular DWM1000 developed by DecaWave [32]; see Section III-A for more details. Recognizing that the nature of the bias generation in the LoS and the NLoS modes are different, we take a two-step approach to our bias correction. First, we use an artificial neural network (ANN), referred to as LaNANN (short for LoS and NLoS ANN), to discriminate the LoS and NLoS measurements. Then, we use a set of two ANNs, LoS bias correction ANN (LBCANN), and NLoS bias correction ANN (NBCANN), to learn the bias-free ranges out of the uncorrected UWB range measurements under LoS and NLoS conditions, respectively. We adopt ANN as our learning model because the universal approximation theorem claims that an ANN with enough depth can approximate any continuous function given certain weights. In other words, we can approximate the complex unknown UWB bias model using the ANN and minimize the size of the ANN to reduce the computational complexity in the mean time. A key feature of our approach is that it is computationally efficient enough to run on a resource-constrained hardware such as small embedded devices as demonstrated in our experimental study.

In most of the existing supervised learning-based bias compensation/correction work such as [33], [34], the ranging bias value acquisition is often assumed trivial and is usually obtained by measuring the ground truth distance between UWB sensors with the tape ruler or the laser tracker and computing the difference between the measured true range and the UWB range measurement. The accuracy of the measured true range directly affects the learning performance. Measuring the true range (ground truth) between UWB sensors by a human can introduce extra errors. The training data for the ML algorithms also often are obtained from stationary sensors. However, in real localization applications, the UWB sensors attached to the targets are maneuvering, which induces potential data mismatch issues due to the additional bias caused by the relative pose of UWB sensors. The relative pose and the antenna radiation patterns of UWB sensors is not often considered in the literature only until some recent work [31], [35]. Even so, these work require bias modeling with respect to the relative pose of the UWB sensors or the access to the relative pose when learning and predicting the bias. And they can only deal with pose-dependent bias due to the limited feature selection. The NLoS scenarios are not included either. In this paper, to collect the training data in both LoS and NLoS conditions, and in a diverse set of relative pose conditions, we use the OptiTrack real-time motion capture system; see Section III-B for details. High precision motion capture camera system [36]–[38] most often are used for engineering purposes such as human gait analysis [39], [40]. The use of this system for applications using UWB ranging is reported in [31] for UWB bias estimation in LoS and in [41] to generate aiding measurements to improve localization of an integrated inertial measurement unit (IMU)/UWB system. In this paper, the motion capture system is used only for training data generation and validating localization performance purposes. Thus, we call our bias correction framework for both LoS and NLoS UWB ranging the OptiTrack aided learning-based UWB bias correction (OLUC).

The rest of the paper is organized as follows. Section II introduces the UWB ranging model. Section III gives the

detail account of our bias correction method depicted in Fig. 1. Finally, Section IV demonstrates the effectiveness of the proposed framework and compares it with the state-of-the-art techniques via a set of UWB pedestrian localization experiments.

## II. Problem Setting

Consider a group of $N$ anchor UWB nodes located at known positions $\{A_1, A_2, \cdots A_N\} \in \mathbf{R}^3$. There is one moving agent with an UWB tag, whose location is denoted by $P_{\text{Tag}} \in \mathbf{R}^3$. This agent can communicate with each of the $N$ anchors and compute the corresponding ToF ranges. The measured range with respect to each anchor consists of the actual distance, the measurement noise, and a bias. Thus, the range measurement $z_n$ between the UWB tag and the $n$-th anchor is computed as follows

$$z_n = \|A_n - P_{\text{Tag}}\|_2 + \omega + b_n, \tag{1}$$

where $\|.\|_2$ is the Euclidean distance, $\omega$ is the zero mean white Gaussian noise and

$$b_n = \begin{cases} b_n^{LoS}, & \text{LoS} \\ b_n^{NLoS}, & \text{NLoS} \end{cases}, \quad n = 1, 2, \cdots, N \tag{2}$$

is the measurement bias whose value differs in the LoS bias and NLoS ranging conditions. The LoS bias exhibits the joint impact of multi-path, relative orientation, and actual distance, while the NLoS bias corresponds to the LoS bias together with the range measurement increment due to the NLoS additional transmission time. The state estimation update rule in terms of the recursive least square (RLS) estimator [42] of the tag location $\hat{P}_{\text{Tag}}^k$ when the range $z_n^k$ between the UWB tag and the $n$-th anchor is obtained at timestamp $k$ is shown as follow:

$$\hat{P}_{\text{Tag}}^k = \hat{P}_{\text{Tag}}^{k-1} + \mathbf{K}^k(z_n^k - \hat{z}_n^k), \tag{3}$$

where $\mathbf{K}^k$ is the estimator gain matrix, $\hat{z}_n = \|A_n - \hat{P}_{\text{Tag}}^{k-1}\|_2$ is the predicted range measurement. Given the biased range measurement model in (1), the estimation error $\mathbf{e}^k$ of the RLS estimator at time $k$ is obtained as

$$\mathbf{e}^k = P_{\text{Tag}}^k - \hat{P}_{\text{Tag}}^k = (\mathbf{I} - \mathbf{K}^k\mathbf{H}^k)\mathbf{e}^{k-1} - \mathbf{K}^k(b_n + \omega), \tag{4}$$

where $\mathbf{I}$ is the identity matrix and $\mathbf{H}^k = \frac{\partial\|A_n - P_{\text{Tag}}\|_2}{\partial P_{\text{Tag}}}|_{P_{\text{Tag}}=\hat{P}_{\text{Tag}}^{k-1}}$. And the location estimation covariance matrix $\mathbf{\Sigma}^k$ at time $k$ is

$$\mathbf{\Sigma}^k = (\mathbf{I} - \mathbf{K}^k\mathbf{H})\mathbf{\Sigma}^{k-1}. \tag{5}$$

As we can infer from (4) and (5), even though the bias $b_n$ does not directly affect the covariance $\mathbf{\Sigma}^k$, it aggravates the location estimation error $\mathbf{e}^k$ instantly. In fact, the bias is ubiquitous in real data. Ignoring the bias mismatches the reality under both Los and NLoS UWB ranging, which leads to inconsistent estimation results. Figure 2 shows the result of an experiment study that compares the raw UWB range measurements with the true distance between UWB sensors. As it can be inferred from Fig. 2, NLoS bias is more significant than the LoS bias in terms of magnitude, while LoS bias cannot be neglected for accurate ranging. A similar observation is reported in our previous work [13] for UWB foot-to-foot ranging where the magnitude of LoS bias is considerable, which motivates us to take LoS bias correction into account for UWB-aided pedestrian localization. The objective of this work is to improve the UWB localization accuracy by determining the LoS and NLoS scenarios and consequently correcting the corresponding bias to generate accurate UWB range measurements using ML techniques.

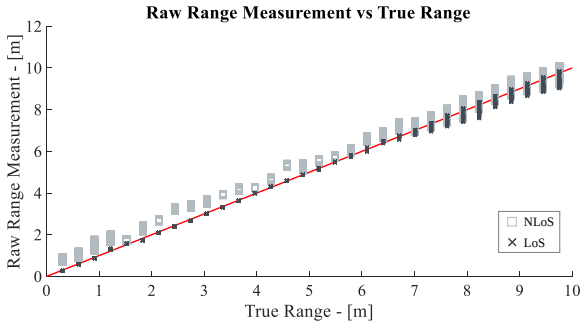


Fig. 2 – The raw UWB range measurements collected at different true distances within 10 m in LoS and NLoS conditions. The measurements are collect by DecaWave DWM1000 UWB sensors described in Section III-B. The red dash-line, regarded as the "ground truth", represents the ideal raw range measurement of the UWB without any error.

## III. Learning-based UWB LoS and NLoS Classification and Bias Correction

This section gives a detailed account of our learning-based bias correction method depicted in Fig. 1.

### A. Feature Analysis and Selection

We focus on designing a bias correction method that can be used with low-cost UWB transceivers. In this study, we use the popular UWB transceiver DWM1000 developed by DecaWave [32] whose data acquisition and ranging software runs on a Teensy 3.2 as shown in the right hand side of Fig. 3. The Teensy 3.2 microcontroller implements a serial peripheral interface protocol to communicate with the UWB and collect sensor measurements [43]. To pick the features for measurement classification and correction, we constrained the choice to the signals that are readily available on this UWB ranging sensor.

We guide our study by the existing results in the literature. To distinguish NLoS UWB measurements from LoS ones, [44] employs a PM-based ranging mode discriminator with a deterministic threshold. The motivation for this choice is that in the LoS condition, the received direct-path signal's power takes a big proportion of the total received signal power. In contrast, in NLoS conditions, the direct path is significantly attenuated or even completely blocked. When the difference between total received power and the direct-path power is larger than a threshold value, [44] argues

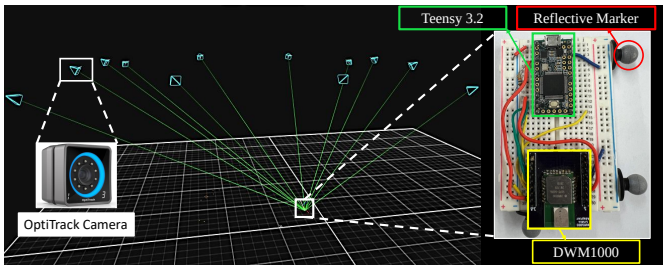


Fig. 3 – The screenshot of tracking the DecaWave DWM1000 UWB sensor attached with reflective markers in the Motive software.

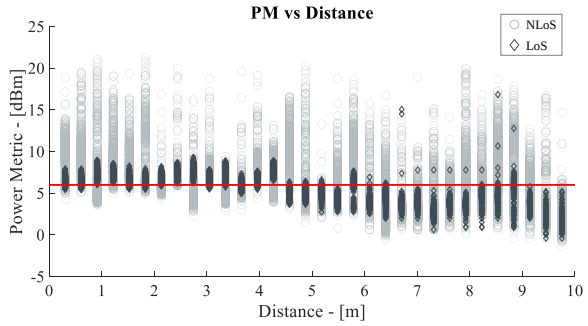


Fig. 4 – The power metric of UWB measurements collected at different distances within 10 m in LoS and NLoS respectively. The red line denotes the deterministic threshold to discriminate LoS and NLoS proposed by [44].

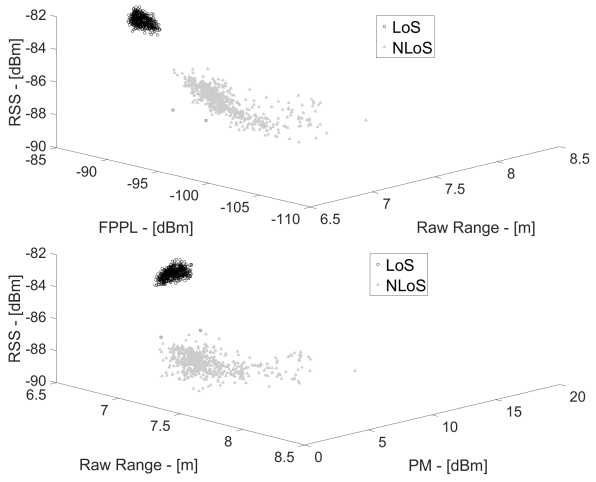


Fig. 5 – The 3-D plot of UWB measurements when true distance between the sensors is 7 m.

that the range measurement can be identified as NLoS. To investigate effectiveness of this feature, we carried out an experimental study at different distances between two UWB sensors under a controlled environment where we know the true measurement scenarios. The results shown in Fig. 4, however indicates that the deterministic threshold represented by the red line cannot completely separate LoS and NLoS measurements, and there is still significant overlapping PM values. By collecting experimental data under various NLoS and LoS ranging condition, in addition to the PM we also included the FPPL and RSS of UWB signals and the raw range

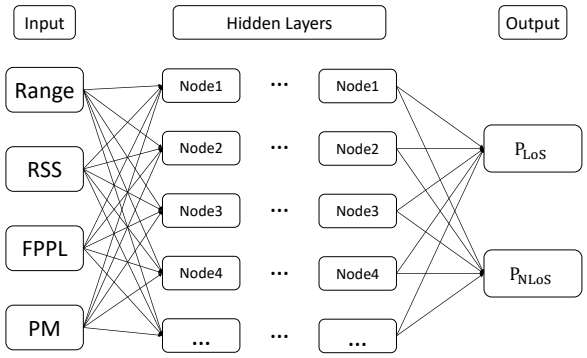


Fig. 6 – The ANN model for UWB LoS and NLoS Classification. The NN structure for learning the range bias looks similar except that at the output layer we have a single neuron for the bias-free range.

measurements as features. For a fixed distance, e.g., 7 m, the 3-D visualization of the UWB measurements under controlled data collection is shown in Fig. 5. As it can be seen in this plot, using these features the LoS and NLoS measurements are more clearly separated from one an other. As we discussed earlier, the relative pose of the transceivers can also effect the ranging bias and thus recent work like [31] considered relative bias as an input feature. However, since obtaining the relative pose is not straightforward and needs additional to the bias correction, because the relative pose is hard to obtain without additional sensors, we did not consider it as a direct feature. However, as our evaluation study for localizing a moving pedestrian in Section IV show our bias correction method delivers high accuracy results despite the varying relative of the transceivers due to the movement. This can be due to the use of a diverse training data that we collect at various relative poses, which provides the opportunity learning of the relative pose-dependent bias implicitly by using signal patterns that can be reflected in FPPL and RSS.

Figure 6 depicts the LaNANN component of our method that is used to classify measurement type. It uses 4 nodes in the input layer corresponding to the UWB measurements of range, RSS, FPPL, and PM while the output layer has 2 nodes for the LoS and NLoS probability, respectively. We use the same input for the two ANNs of LoS and NLoS bias correction in parallel, but their output layers only have 1 node of the bias-free UWB range. In general, the LoS and NLoS scenarios of the UWB measurement can be modeled as a random variable $\theta$ with a Bernoulli distribution mathematically whose probability mass function is as follow

$$f(\theta; p) = \begin{cases} p, & \text{if } \theta = \text{LoS} \\ 1-p, & \text{if } \theta = \text{NLoS} \end{cases} \tag{6}$$

The probability of LoS $p$, as well as the bias-free range $\tilde{z}_n = \|A_n - P_{\text{Tag}}\|_2 + \omega$, based on our selection of the features, are functions of range, RSS, FPPL and PM, respectively.

$$p = f_{\text{LaN}}(\text{range}, \text{RSS}, \text{FPPL}, \text{PM}), \tag{7a}$$

$$\tilde{z}_n = f_{\text{BC}}(\text{range}, \text{RSS}, \text{FPPL}, \text{PM}). \tag{7b}$$

Then our objective boils down to use ANNs to approximate these functions without explicitly know the exact mathematical

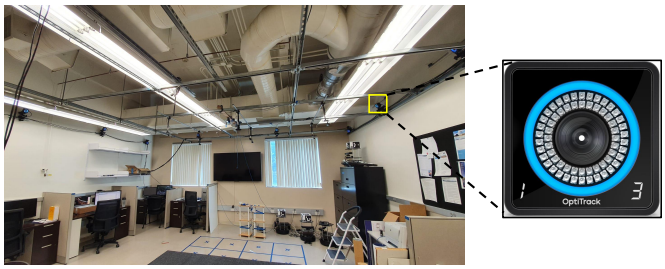


Fig. 7 – The OptiTrack motion capture system in KCS lab at University of California Irvine. The cameras have $1280 \times 1024$ resolution with a 120 Hz native frame rate.

relations.

$$\hat{p} = \hat{f}_{\text{LaNANN}}(\text{range}, \text{RSS}, \text{FPPL}, \text{PM}), \tag{8a}$$

$$\hat{\tilde{z}}_n = \begin{cases} \hat{f}_{\text{LBCANN}}(\text{range}, \text{RSS}, \text{FPPL}, \text{PM}), & \text{if } \hat{p} \geq 0.5 \\ \hat{f}_{\text{NBCANN}}(\text{range}, \text{RSS}, \text{FPPL}, \text{PM}), & \text{if } \hat{p} < 0.5 \end{cases}. \tag{8b}$$

where $\hat{f}_{\text{LaNANN}}$, $\hat{f}_{\text{LBCANN}}$ and $\hat{f}_{\text{NBCANN}}$ denotes the generic functions of the feed-forward LaNANN, LBCANN and NBCANN respectively.

### B. OptiTrack-aided Training Data Generation

Generating the training data of ANNs for LoS and NLoS classification and the corresponding bias correction is not a trivial task. Traditionally, the UWB sensors are placed statically at known locations where the actual reference range between UWB sensors can be measured or calculated. The accuracy of the reference range highly depends on the precision of the location and the measurements. The success of ML-based methods depends on extensive and informative training data generation, otherwise, the out-of-sample performance cannot be guaranteed due to the distributional mismatch. UWB ranging is often is used for moving target localization. Using data generated in stationary configurations lacks diversity of relative pose that is often the case when we track a moving object. As we mentioned in Section III-A, we proposed to incorporate the relative pose implicitly in the measurements, therefore, we have to make our training data set contain as many relative-poses as possible. Collecting training data manually at various relative-poses is not feasible since there are infinite amount of relative-poses. Therefore, to obtain more abundant training data and reduce the difference between the training and the test data set, we use the OptiTrack motion capture camera system to obtain an accurate bias-free range in a dynamical manner.

The OptiTrack system is a precise motion capture and 3-D tracking system with a localization error of less than $0.2$ mm via optical ranging and trilateration for numerous applications, e.g., video game design, virtual reality, and robotics. The OptiTrack system in our KCS lab is shown in Fig. 7. The cameras can precisely perceive the particular reflective markers' location via visual-based ranging techniques. As such, we attach at least 3 reflective markers on the UWB sensors so that they form a rigid body that can be recognized and tracked by the OptiTrack system as shown in Fig. 3 which exhibits the track of a UWB sensor in the associated OptiTrack software called Motive.

The pivot point of the UWB rigid body defined by the reflective markers can be manually assigned and tracked. Consequently, we can obtain the accurate position of the UWB sensors by setting their antennas as the pivot points and then calculate explicitly the distances between the pivot points as the label values, i.e., bias-free ranges, for the ANN model. The advantage of this approach to measure the actual distances is that the UWB sensors are not necessarily fixed at certain locations. Instead, the UWB sensors can be attached or carried by any moving objects or agents, while the UWB sensors can provide their own measurements in the meantime as the input features go into the ANN. To generate a diverse and abundant training data set, in our study case, an agent holding a Tag UWB sensor that connects to three anchor UWB sensors randomly walks under the OptiTrack systems in the LoS condition in our KCS lab for $5$ minutes. The agent also waves the Tag UWB in the air to make different relative poses and collects various measurements to the full extent that contains biased ones caused by other factors illustrated before. All collected data are labeled by LoS. For NLoS cases, we put various obstacles found in our lab space between the Tag and the anchors and repeat the same data collection procedure as in LoS. The OptiTrack-aided training data generation experiment is illustrated in Fig. 8. One assumption made here is that the effect of the UWB relative pose, NLoS and multi-path on the range bias is encoded intangibly in the power features of the UWB signals, i.e., PM, FPPL, and RSS, that can be learned by the ANN model. In conclusion, by collecting data in such a dynamical setting, we can enrich the training data set without collecting the relative pose data explicitly and reduce the distributional difference between the training data and the test data to a considerable extent.

### C. Training Result

The UWB device we used to generate the training data is DecaWave DWM1000 and the sampling rate was set to $10$ Hz. We generated $300000$, $150000$, and $150000$ samples of the UWB range, PM, FPPL, RSS, and bias-free range for the LaNANN, LBCANN, and NBCANN, respectively, via agent random walks conducted in the KCS lab at UC, Irvine. The samples are split into a training set, a validation set and a test set according to the ratio of $70\%$, $15\%$, and $15\%$. For the LaNANN, the label is LoS $(0)$ and NLoS $(1)$, while that of LBCANN and NBCANN is the bias-free range. We used the grid search method [45], [46] to tune the hyperparameters of all ANNs during the training process. The fine-tuned design of all three ANNs is shown in Table I.

In summary, the training results are shown in Table. II where the best classification accuracy in test sets achieved by LaNANN is $92.73\%$. Also, the root mean square error (RMSE) for the test set for LBCANN and NBCANN is $0.1351$ m and

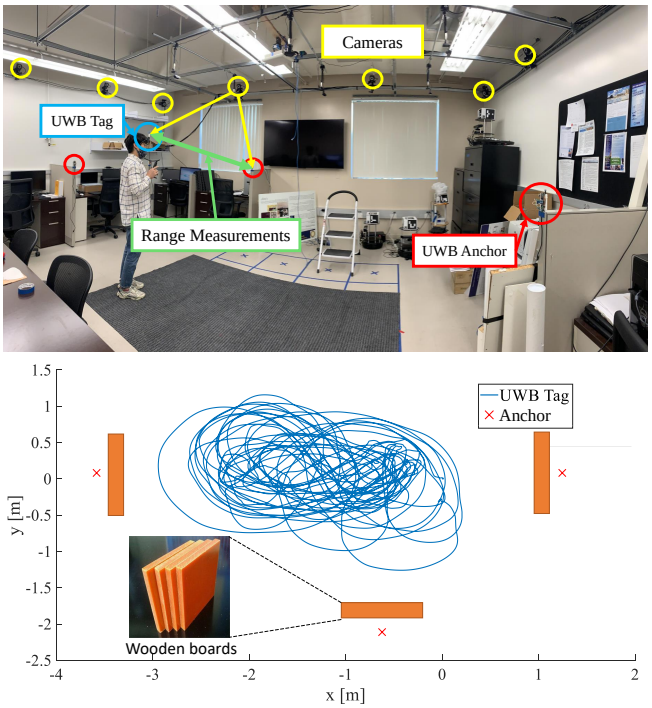


Fig. 8 – The OptiTrack-aided training data generation experiment where the agent holding a Tag UWB sensor walks along a random trajectory. The reference position of all UWB sensors are obtained by the OptiTrack. The blue line denotes the trajectory of the Tag UWB while the red crosses represent the anchors. For NLoS data collection, multiple obstacles such as wooden boards (shown as the orange rectangles) and human body are placed to block the direct path between the Tag and anchors.

| Hyperparameters | LaNANN | LBCANN | NBCANN |
|---|---|---|---|
| Number of hidden layers | 2 | 3 | 3 |
| Number of units per layer | 10 | 11 | 18 |
| Loss | Cross-Entropy | MSE | MSE |
| Activation function | Sigmoid | ReLU | ReLU |
| Optimizer | Adam | Adam | Adam |
| Batch size | 256 | 512 | 512 |
| Learning rate | 0.05 | 0.025 | 0.025 |

TABLE I – The hyperparameter design of the ANNs.

| | Training | Validation | Test |
|---|---|---|---|
| LaNANN (Accuracy: %) | 94.39 | 94.12 | 92.73 |
| LBCANN (RMSE: m) | 0.1308 | 0.1316 | 0.1351 |
| NBCANN (RMSE: m) | 0.1557 | 0.1563 | 0.1662 |

TABLE II – The summary of training result for all ANNs.

0.1662 m, respectively. As for the computational perspective, the training period took around 2 hour in total while the prediction run time for LaNANN, LBCANN and NBCANN is 0.0022 ms, 0.0029 ms and 0.0041 ms using a Dell Laptop: Intel Core$^{TM}$ i5-1135G7@4.20GHz, quad-core, 8 GB memory.

## IV. Experimental Evaluations

To verify the effectiveness of our ANNs for UWB bias correction, we implemented our model, which was well-trained using the data in Section III-B in another set of localization experiments conducted in the Public Safety Immersive Test Center (PSITC), a collaboration between the First Responder Network Authority and the National Institute of Standards and Technology's Public Safety Communications Research Division, located in Boulder, CO. One agent with a Tag UWB sensor walked along three different trajectories, i.e., straight lines, rectangles, and lemniscates (Figure-8 shape), for around 5 minutes, as depicted in Fig. 9. Each trajectory was repeated three times. Three additional UWB anchors are placed at known locations maintaining the communication with the Tag. Due to the block of human bodies, roadblocks and walls in the testing venue, the measurement scenarios were constantly switching between Los and NLoS. We used the OptiTrack system installed in the PSITC facility to provide high-accuracy reference trajectories for comparison. Note that the reference trajectories were used for the evaluation of our bias correction method rather than training any new model. During the experimental evaluations, we made an inductive bias to the ANNs that for the consecutive predictions given by the ANNs cannot abruptly change within a small time period since the actual ranges between the Tag and anchors are continuous and the LoS and NLoS switching is less frequent. We put some weight on the previous prediction so that during real-time implementation the predicted bias-free range by the ANNs is smoothed, which is equivalent to the moving average method in terms of the format. Additionally, we selected the RLS method for the location estimation of the agent and removed the faulty measurements (extreme values).

For comparison study, we also trained another ANN set using the same features but using a data set that was collected in limited number of stationary configurations and the true distances were measured by human using measuring tape. We compared our proposed OLUC method with this so-called "stationary-ANN" method. We also compared the effectiveness of our bias correction method for localization with the OptiTrack aided method proposed in [41] which uses an ANN method to fuse IMU/UWB based localization with Optitrack measurements to improve localization accuracy. We called this method "ANN fusion". And we trained and evaluated its ANN based on the same trajectories according to [41] to make a fair comparison with our proposed method. The experimental results are shown in Fig. 10 and Fig. 11. Lastly, in order to test the generalization of our proposed method against the "ANN fusion" on unseen new data, we additionally conducted a set of localization experiments in the CALIT2 building at UC Irvine, where the OptiTrack is not available and the LoS/NLoS conditions are more complicate due to the cubicles in the environments as shown in Fig. 12. The experimental settings other than the designed trajectory remained the same as previous ones. Note that in this extra experiment, we tested the fusion ANN via a new trajectory on which it was not trained. Fig. 13 and Table III illustrate the additional comparison results. We used the loop-closure error for the mobile UWB tag instead of the RMSE since its start and end point are identical and the reference is less accurate.

As it can be directly seen from the estimated agent's trajectories in Fig. 10, after applying our proposed OLUC

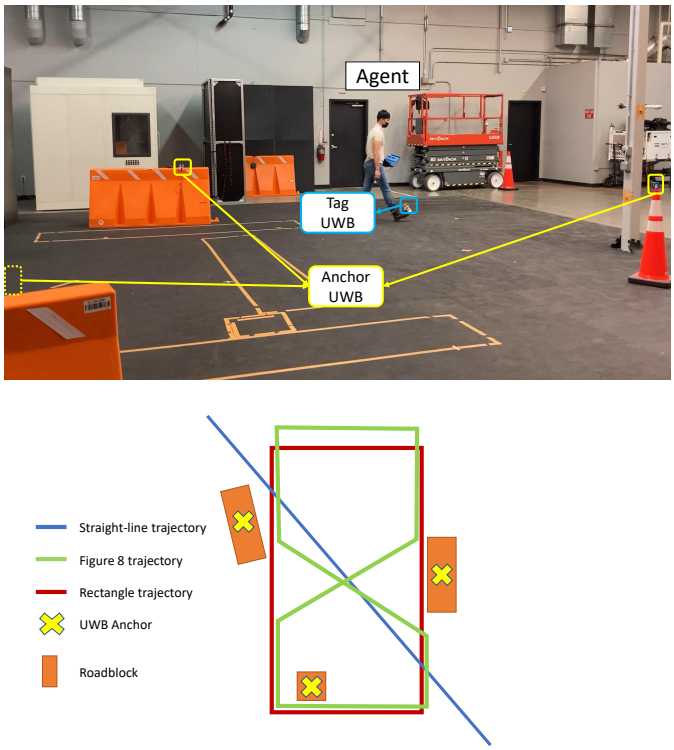


Fig. 9 – The demonstration experiments conducted in the PSITC facility associated with the bottom diagram that shows the designed trajectories of the mobile UWB tag, the positions of the anchors, and of the obstacle roadblocks.

| | Raw | Proposed | ANN Fusion |
|---|---|---|---|
| Loop-Closure Error (m) | 0.8046 | 0.2643 | 1.5020 |

TABLE III – The loop-closure error of the trajectory using the proposed method versus the ANN fusion.

method to correct UWB range bias in LoS and NLoS hybrid environment, the localization accuracy of the moving agent using the RLS method is significantly improved. The error plots, as well as the performance metrics in Fig. 11, demonstrate that our OLUC method achieved substantial bias reduction rates of 66.91%, 64.66%, and 63.13%, in the three scenarios that we considered. Note that the stationary ANN has an inferior performance due to the out-of-sample problem that we discussed earlier. As for the ANN Fusion method in [41], it has similar performance as our proposed OLUC. However, it works only when the OptiTrack is available or the training and the evaluation trajectories are the same. Because it necessarily needs to train the ANN based on the estimated position obtained by both the UWB sensors and the OptiTrack rather than the UWB signal, which makes the generalization performance not satisfactory. We can obtain above conclusion from both Fig. 13 showing the trajectories and Table III comparing the loop-closure errors as they show that the ANN fusion performs even worse than using the raw measurements. But our proposed method still performed well. Therefore, the ANN Fusion method is only a position enhancement using and highly dependent on the OptiTrack and has limitation in generalization. If the OptiTrack is not available and the designed trajectory is not seen by the ANN, it fails easily. On the contrary, our proposed OLUC does not highly rely on the OptiTrack, since we only used the OptiTrack to generate training data. The evaluation using the OptiTrack is not a necessity.

## V. Conclusions

UWB ranging bias correction has a significant impact on localization accuracy of the navigation algorithms that use UWB ranging. In this paper, we addressed the problem of UWB ranging bias correction in complex localization scenarios by training neural network models to distinguish LoS and NLoS scenarios and predict the corresponding bias-free range in real-time using features that are readily available on low-cost UWB sensor. Our experimental data collection resulted in identifying a novel set of features, raw range, PM, FPPL and RSS, to train ANNs for measurement type classification and bias-free range prediction. The effectiveness of any learning-based solution depends on diversity and informativeness of its training data. Recognizing that the relative orientation of ranging sensor affects the ranging accuracy, we used an Optitrack motion capture system to collect high accuracy ranging between a tag on a moving agent and fixed UWB anchor nodes. In doing so, we collected a diverse set of data in various relative poses between the sensors. The effectiveness of our OptiTrack-aided supervised learning-based UWB bias correction method was demonstrated via a set of pedestrian localization experiments using the RLS algorithm for location estimation. Our experiments showed that our method leads to a considerable improvement in the localization accuracy.

## Acknowledgment

The authors thank Joe Grasso from NIST and Chico (Chi-Shih) Jao and Minwon Seo from UCI for assisting with the experimental data collection.

## References

[1] F. Zafari, A. Gkelias, and K. K. Leung, "A survey of indoor localization systems and technologies," *IEEE Communications Surveys & Tutorials*, vol. 21, no. 3, pp. 2568–2599, 2019.

[2] F. Mazhar, M. G. Khan, and B. Sällberg, "Precise indoor positioning using UWB: A review of methods, algorithms and implementations," *Wireless Personal Communications*, vol. 97, no. 3, pp. 4467–4491, 2017.

[3] D. Feng, C. Wang, C. He, Y. Zhuang, and X.-G. Xia, "Kalman-filter-based integration of IMU and UWB for high-accuracy indoor positioning and navigation," *IEEE Internet of Things Journal*, vol. 7, no. 4, pp. 3133–3146, 2020.

[4] O. P. Kumar, P. Kumar, T. Ali, P. Kumar, and S. Vincent, "Ultrawideband antennas: Growth and evolution," *Micromachines*, vol. 13, no. 1, p. 60, 2021.

[5] D. Wang, S. Yoo, and S. H. Cho, "Experimental comparison of IR-UWB radar and FMCW radar for vital signs," *Sensors*, vol. 20, no. 22, p. 6695, 2020.

[6] K. Han and S. Hong, "Phase-extraction method with multiple frequencies of fmcw radar for human body motion tracking," *IEEE Microwave and Wireless Components Letters*, vol. 30, no. 9, pp. 927–930, 2020.

[7] N. Kumchaiseemak, I. Chatnuntawech, S. Teerapittayanon, P. Kotchapansompote, T. Kaewlee, M. Piriyajitakonkij, T. Wilaiprasitporn, and S. Suwajanakorn, "Toward ant-sized moving object localization using deep learning in fmcw radar: A pilot study," *IEEE Transactions on Geoscience and Remote Sensing*, vol. 60, pp. 1–10, 2022.

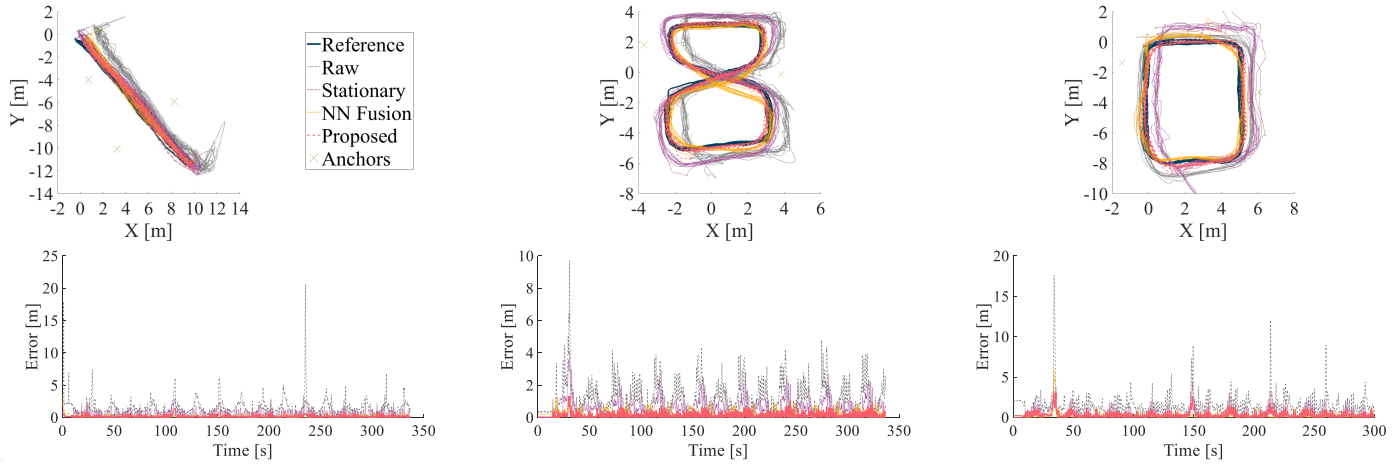


(a) Straight Line (b) Figure 8 (c) Rectangle

Fig. 10 – The estimated trajectories of the agent using RLS localization method as well as the localization error plots before bias correction (using raw measurements) and after applying different bias correction methods, i.e., stationary-ANN method, ANN Fusion and the proposed OLUC.

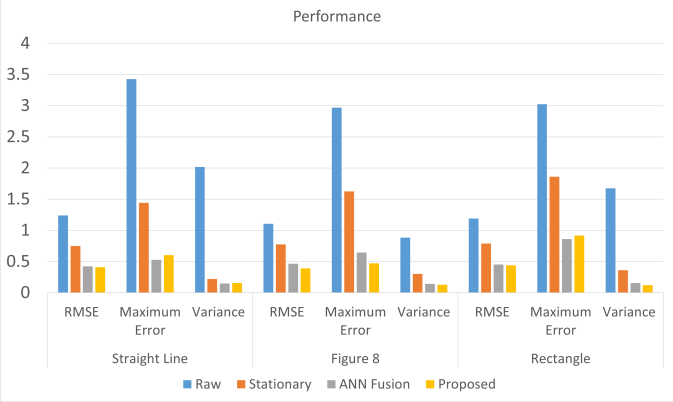


Fig. 11 – The average experimental statistics of the different trajectories using different bias correction methods.

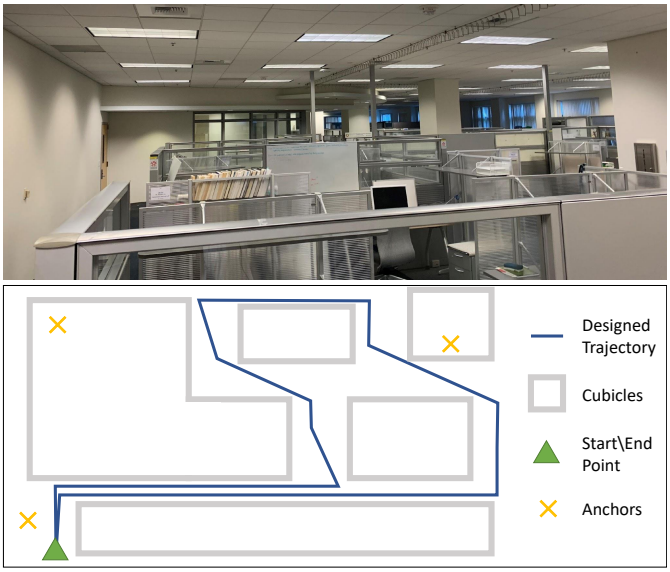


Fig. 12 – The demonstration experiments conducted in the cubicle environment in the CALIT2 building at UC Irvine associated with the bottom diagram that shows the designed trajectories of the mobile UWB tag, the start and end point, the positions of the anchors, and of the cubicle configurations.

[8] A. Poulose and D. S. Han, "UWB indoor localization using deep learning LSTM networks," *Applied Sciences*, vol. 10, no. 18, p. 6290, 2020.
[9] T. H. Nguyen, T.-M. Nguyen, and L. Xie, "Range-focused fusion of camera-IMU-UWB for accurate and drift-reduced localization," *IEEE Robotics and Automation Letters*, vol. 6, no. 2, pp. 1678–1685, 2021.
[10] M.-W. Seo and S. S. Kia, "Online target localization using adaptive belief propagation in the HMM framework," *IEEE Robotics and Automation Letters*, vol. 7, no. 4, pp. 10288–10295, 2022.
[11] K. Yu, K. Wen, Y. Li, S. Zhang, and K. Zhang, "A novel NLoS mitigation algorithm for UWB localization in harsh indoor environments," *IEEE Transactions on Vehicular Technology*, vol. 68, no. 1, pp. 686–699, 2018.
[12] A. Musa, G. D. Nugraha, H. Han, D. Choi, S. Seo, and J. Kim, "A decision tree-based NLoS detection method for the UWB indoor location tracking accuracy improvement," *International Journal of Communication Systems*, vol. 32, no. 13, p. e3997, 2019.
[13] C. Chen, C.-S. Jao, A. M. Shkel, and S. S. Kia, "UWB sensor placement for foot-to-foot ranging in dual-foot-mounted ZUPT-aided INS," *IEEE Sensors Letters*, vol. 6, no. 2, pp. 1–4, 2022.
[14] J. Chen, D. Raye, W. Khawaja, P. Sinha, and I. Guvenc, "Impact of 3D UWB antenna radiation pattern on air-to-ground drone connectivity," in *Vehicular Technology Conference*, pp. 1–5, 2018.
[15] K. Wen, K. Yu, and Y. Li, "NLoS identification and compensation for UWB ranging based on obstruction classification," in *European Signal Processing Conference*, pp. 2704–2708, 2017.
[16] N. Rajagopal, P. Lazik, N. Pereira, S. Chayapathy, B. Sinopoli, and A. Rowe, "Enhancing indoor smartphone location acquisition using floor plans," in *ACM/IEEE International Conference on Information Processing in Sensor Networks*, pp. 278–289, 2018.
[17] Z. Zeng, S. Liu, and L. Wang, "UWB/IMU integration approach with NLOS identification and mitigation," in *2018 52nd Annual Conference on Information Sciences and Systems (CISS)*, pp. 1–6, IEEE, 2018.
[18] A. Musa, G. D. Nugraha, H. Han, D. Choi, S. Seo, and J. Kim, "A decision tree-based NLOS detection method for the UWB indoor location tracking accuracy improvement," *International Journal of Communication Systems*, vol. 32, no. 13, p. e3997, 2019.
[19] A. D. Preter, G. Goysens, J. Anthonis, J. Swevers, and G. Pipeleers, "Range bias modeling and autocalibration of an UWB positioning system," in *2019 International Conference on Indoor Positioning and*

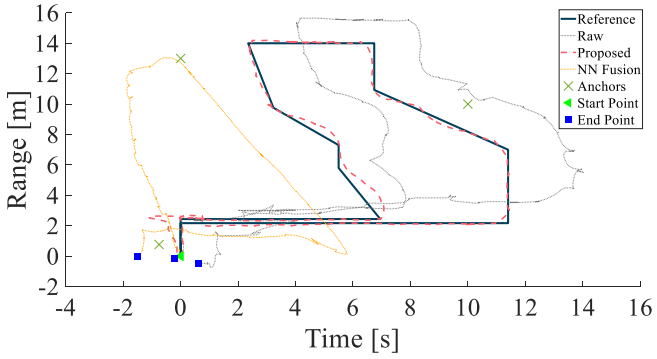


Fig. 13 – The estimated trajectory of the mobile UWB tag using the proposed OLUC method and the ANN fusion.

*Indoor Navigation*, pp. 1–8, 2019.

[20] J. Bluemel, A. Fornasier, and S. Weiss, "Bias compensated UWB anchor initialization using information-theoretic supported triangulation points," in *2021 IEEE International Conference on Robotics and Automation (ICRA)*, pp. 5490–5496, 2021.

[21] J. Cano, G. Pages, E. Chaumette, and J. Le Ny, "Clock and power-induced bias correction for UWB time-of-flight measurements," *IEEE Robotics and Automation Letters*, 2022.

[22] S. Y. Cho, "Two-step calibration for UWB-based indoor positioning system and positioning filter considering channel common bias," *Measurement Science and Technology*, vol. 30, no. 2, p. 025003, 2018.

[23] J. Zhu and S. S. Kia, "Bias compensation for UWB ranging for pedestrian geolocation applications," *IEEE Sensors Letters*, vol. 3, no. 9, pp. 1–4, 2019.

[24] B. van der Heijden, A. Ledergerber, R. Gill, and R. D'Andrea, "Iterative bias estimation for an ultra-wideband localization system," *IFAC-PapersOnLine*, vol. 53, no. 2, pp. 1391–1396, 2020.

[25] J. Zhu and S. S. Kia, "Decentralized cooperative localization with LoS and NLoS UWB inter-agent ranging," *IEEE Sensors Journal*, vol. 22, no. 6, pp. 5447–5456, 2021.

[26] W. Zhao, A. Goudar, and A. P. Schoellig, "Finding the right place: Sensor placement for UWB time difference of arrival localization in cluttered indoor environments," *IEEE Robotics and Automation Letters*, vol. 7, no. 3, pp. 6075–6082, 2022.

[27] J. B. Kristensen, M. M. Ginard, O. K. Jensen, and M. Shen, "Non-line-of-sight identification for UWB indoor positioning systems using support vector machines," in *2019 IEEE MTT-S International Wireless Symposium (IWS)*, pp. 1–3, IEEE, 2019.

[28] R. Qi, X. Li, Y. Zhang, and Y. Li, "Multi-classification algorithm for human motion recognition based on IR-UWB radar," *IEEE Sensors Journal*, vol. 20, no. 21, pp. 12848–12858, 2020.

[29] L. Schmid, D. Salido-Monzú, and A. Wieser, "Accuracy assessment and learned error mitigation of UWB ToF ranging," in *2019 International Conference on Indoor Positioning and Indoor Navigation*, pp. 1–8, 2019.

[30] V. Barral, C. J. Escudero, J. A. García-Naya, and R. Maneiro-Catoira, "NLoS identification and mitigation using low-cost UWB devices," *Sensors*, vol. 19, no. 16, p. 3464, 2019.

[31] W. Zhao, J. Panerati, and A. P. Schoellig, "Learning-based bias correction for time difference of arrival ultra-wideband localization of resource-constrained mobile robots," *IEEE Robotics and Automation Letters*, vol. 6, no. 2, pp. 3639–3646, 2021.

[32] A. Alarifi, A. Al-Salman, M. Alsaleh, A. Alnafessah, S. Al-Hadhrami, M. Al-Ammar, *et al.*, "Decawave DWM1000 module," *Available online: https://www.decawave.com/product/dwm1000-module/*.

[33] M. A. Shalaby, C. C. Cossette, J. R. Forbes, and J. L. Ny, "Calibration and uncertainty characterization for ultra-wideband two-way-ranging measurements," *arXiv preprint arXiv:2210.05888*, 2022.

[34] S. Angarano, V. Mazzia, F. Salvetti, G. Fantin, and M. Chiaberge, "Robust ultra-wideband range error mitigation with deep learning at the edge," *Engineering Applications of Artificial Intelligence*, vol. 102, p. 104278, 2021.

[35] A. Ledergerber and R. D'andrea, "Calibrating away inaccuracies in ultra wideband range measurements: A maximum likelihood approach," *IEEE Access*, vol. 6, pp. 78719–78730, 2018.

[36] A. Chan, J. Aguillon, D. Hill, and E. Lou, "Precision and accuracy of consumer-grade motion tracking system for pedicle screw placement in pediatric spinal fusion surgery," *Medical engineering & physics*, vol. 46, pp. 33–43, 2017.

[37] J. S. Furtado, H. H. Liu, G. Lai, H. Lacheray, and J. Desouza-Coelho, "Comparative analysis of Optitrack motion capture systems," in *Advances in Motion Sensing and Control for Robotic Applications*, pp. 15–31, Springer, 2019.

[38] J. Jiao, H. Wei, T. Hu, X. Hu, Y. Zhu, Z. He, J. Wu, J. Yu, X. Xie, H. Huang, *et al.*, "Fusionportable: A multi-sensor campus-scene dataset for evaluation of localization and mapping accuracy on diverse platforms," *arXiv preprint arXiv:2208.11865*, 2022.

[39] L. Ruiz-Ruiz, F. Seco, A. Jiménez, S. Garcia, and J. J. García, "Evaluation of gait parameter estimation accuracy: a comparison between commercial IMU and optical capture motion system," in *2022 IEEE International Symposium on Medical Measurements and Applications*, pp. 1–2, 2022.

[40] S. P. Savić, B. Ristić, N. Prodanović, and G. Devedzić, "Comparative gait analysis of parameters of the knee joint after CR and PS implantations," in *2022 11th Mediterranean Conference on Embedded Computing*, pp. 1–4, 2022.

[41] A. M. Almassri, N. Shirasawa, A. Purev, K. Uehara, W. Oshiumi, S. Mishima, and H. Wagatsuma, "Artificial neural network approach to guarantee the positioning accuracy of moving robots by using the integration of IMU/UWB with motion capture system data fusion," *Sensors*, vol. 22, no. 15, p. 5737, 2022.

[42] Y. Bar-Shalom, X. Li, and T. Kirubarajan, *Estimation with applications to tracking and navigation: theory algorithms and software*. John Wiley & Sons, 2004.

[43] P. Stoffregen, "Teensy 3.2 datasheet." `https://www.pjrc.com/teensy/techspecs.html`, 2016. Accessed: March 17, 2023.

[44] K. Gururaj, A. K. Rajendra, Y. Song, C. L. Law, and G. Cai, "Real-time identification of NLoS range measurements for enhanced UWB localization," in *International Conference on Indoor Positioning and Indoor Navigation*, pp. 1–7, 2017.

[45] J.-M. Dufour and J. Neves, "Finite-sample inference and nonstandard asymptotics with Monte Carlo tests and R," in *Handbook of statistics*, vol. 41, pp. 3–31, Elsevier, 2019.

[46] R. Khalid and N. Javaid, "A survey on hyperparameters optimization algorithms of forecasting models in smart grid," *Sustainable Cities and Society*, vol. 61, p. 102275, 2020.